



Induced magnetosphere and its outer boundary at Venus

T. L. Zhang,^{1,2} M. Delva,¹ W. Baumjohann,¹ M. Volwerk,¹ C. T. Russell,³ H. Y. Wei,³ C. Wang,² M. Balikhin,⁴ S. Barabash,⁵ H.-U. Auster,⁶ and K. Kudela⁷

Received 4 June 2008; revised 11 August 2008; accepted 29 September 2008; published 20 December 2008.

[1] The induced magnetosphere at Venus consists of regions near the planet and its wake for which the magnetic pressure dominates all other pressure contributions. Initial Venus Express measurements indicate a well-defined outer boundary, the magnetopause, of the induced magnetosphere. This magnetopause acts as an obstacle to deflect the solar wind. Across this boundary, the magnetic field exhibits abrupt directional changes and pronounced draping. In this paper, we examine the structure of the magnetopause using Venus Express magnetic measurements. We find that the magnetopause is a directional discontinuity resembling either a tangential or a rotational discontinuity depending on the interplanetary magnetic field orientation.

Citation: Zhang, T. L., et al. (2008), Induced magnetosphere and its outer boundary at Venus, *J. Geophys. Res.*, 113, E00B20, doi:10.1029/2008JE003215.

1. Introduction

[2] It is well known that the solar wind interaction with a planet produces a magnetosphere-like structure near the planet with common features such as bow shock, magnetosheath, magnetotail, and boundary layers. These magnetosphere-like structures are found at all planets in the solar system regardless if the planet has an intrinsic global magnetic field or not. In the case of planets like Mercury, Earth, Jupiter, Saturn, Uranus and Neptune, a magnetosphere is formed by the interaction of the solar wind with the planet's large intrinsic magnetic field. For a planet like Venus or Mars, which has no global intrinsic magnetic field but with atmosphere, an induced magnetosphere is created by the solar wind interaction with the highly conducting ionosphere. The induced magnetosphere is therefore analogous to the magnetosphere of an intrinsically magnetized planet, but occupies a smaller volume.

[3] The term "induced magnetosphere," to our knowledge, was coined first by *Podgorny et al.* [1980] in describing the solar wind interaction with comets and Venus. *Ness et al.* [1982] used this term in studying the interaction between Titan and the Saturnian magnetospheric flow. The induced magnetosphere was used because although

there is no intrinsic magnetic field at Titan, it possesses a magnetotail with similar configuration as the magnetotail produced from an intrinsic magnetic field. Further, *Ness et al.* [1982] called the outer boundary of the induced magnetosphere the magnetopause.

[4] Recently, *Luhmann et al.* [2004] revitalized the term-induced magnetosphere by giving it a global picture. *Luhmann et al.* [2004] gave a working definition of an induced magnetosphere as "everything between an outer boundary outside of which the obstacle has no effect on the external medium, and an inner boundary inside of which there is no effect of the external conditions." The term-induced magnetosphere has been widely used by the recent Venus Express publications [*Barabash et al.*, 2007; *Zhang et al.*, 2007; *Kallio et al.*, 2008; *Fedorov et al.*, 2008]. *Zhang et al.* [2007] further updated the definition of the induced magnetosphere to be the regions near the planet and its wake in which magnetic pressure dominates the other pressure contributions. Figure 1 illustrates the current understanding of Venus induced magnetosphere and its boundaries. The outer boundary of the induced magnetosphere is the magnetopause and the inner boundary is the ionopause. The dayside portion of the induced magnetosphere is often called the magnetic barrier and the nightside portion of the induced magnetosphere the magnetotail.

[5] *Russell et al.* [1979] noticed that the magnetic field piles up to form a magnetic barrier in the inner magnetosheath on the dayside from the initial observations of Pioneer Venus Orbiter (PVO). *Zhang et al.* [1991] found that the magnetic barrier acts as an obstacle to the solar wind in analogy to the Earth's magnetosphere. They found that the magnetic barrier is bounded by the ionopause as the lower boundary and a pressure balanced magnetic barrier upper boundary.

[6] An initial survey of the Venus Express (VEX) magnetic field time series data indicates a well-defined boundary, the magnetopause, located at the outer edge of the magnetic barrier region [*Zhang et al.*, 2007]. This magne-

¹Space Research Institute, Austrian Academy of Sciences, Graz, Austria.

²State Key Laboratory of Space Weather, Center for Space Science and Applied Research, Chinese Academy of Sciences, Beijing, China.

³Institute of Geophysics and Planetary Physics, University of California, Los Angeles, California, USA.

⁴Department of Automatic Control and Systems Engineering, University of Sheffield, Sheffield, UK.

⁵Swedish Institute of Space Physics, Kiruna, Sweden.

⁶Institut für Geophysik und Extraterrestrische Physik, Technische Universität, Braunschweig, Germany.

⁷Institute of Experimental Physics, Slovak Academy of Sciences, Košice, Slovakia.

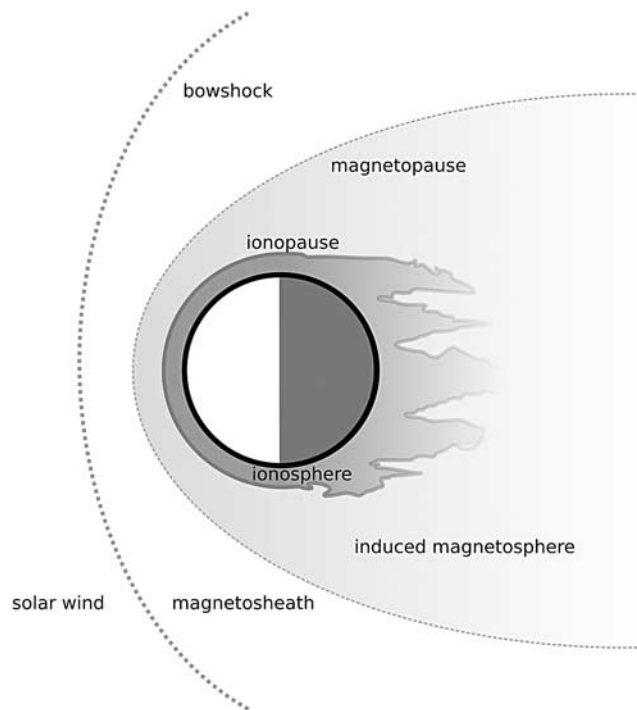


Figure 1. Schematic of Venus induced magnetosphere and its boundaries.

topause is easily identified as a sudden cessation of magnetosheath wave activity and an abrupt start of pronounced field draping in the inner magnetosheath where the field magnitude is enhanced. The magnetic barrier, an induced magnetosphere on the dayside, is found with the same thickness at both solar minimum and solar maximum [Zhang *et al.*, 2008a]. Finally, it was found that the magnetopause has no signature in the field magnitude and the thickness is about 200 km in vertical extent. It is the purpose of this paper to present a more detailed analysis of the magnetic field data on the induced magnetosphere and its outer boundary. A complete description of the induced magnetosphere will require a combination of all relevant magnetic and plasma data. However, at time of writing, the plasma moment data are still not available, thus we restrict our analysis to the magnetic field data only.

2. Instrumentation and Data

[7] The Venus Express mission is the first European mission to Venus [Titov *et al.*, 2006]. The spacecraft has a highly elliptical polar orbit with a period of 24 h. Among other instruments, it carries a magnetometer to investigate the Venus plasma environment [Zhang *et al.*, 2006]. The Venus Express magnetometer (MAG) consists of two triaxial fluxgate sensors. Because of schedule and budget constraint, no magnetic cleanliness program was implemented. The outboard sensor is mounted to the tip of a one meter deployable boom whereas the inboard sensor is directly attached to the top panel of the spacecraft. The magnetometer is designed using dual sensor or gradiometer method [Ness *et al.*, 1971]. Both sensors sample simultaneously, to enable separation of spacecraft originated stray field effects from the ambient space field. The instrument has been

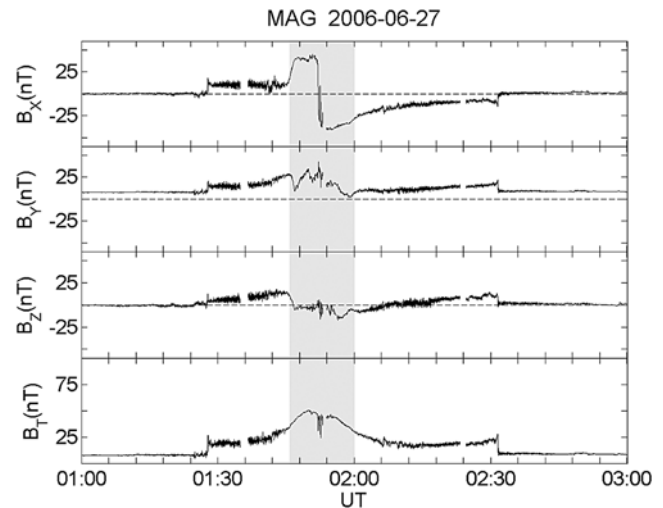


Figure 2. Magnetic field measurements around periapsis (0153 UT, altitude is 302 km, SZA is 88.8°) on 27 June 2006. The shadowed area is the induce magnetosphere.

carefully designed to cope with this great challenge of a “dirty” spacecraft with a large dynamic range, large automatic compensation range, and high digital resolution.

[8] We process and clean the data based on dual-sensor measurements. The detailed description of the data cleaning method can be found by Zhang *et al.* [2008b]. Basically, we examine the time series ΔB , of the differences of the inboard and outboard magnetic field measurements in

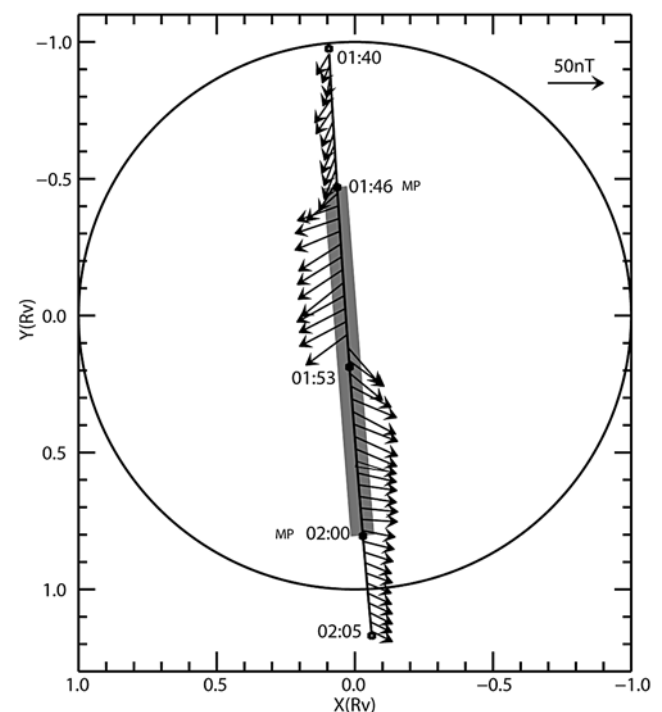


Figure 3. The magnetic field in VSO coordinates plotted along the trajectory through the induced magnetosphere on 27 June 2006. The thick line marks the induced magnetosphere part of the trajectory. Magnetopause crossings are indicated at 0146 and 0200 UT.

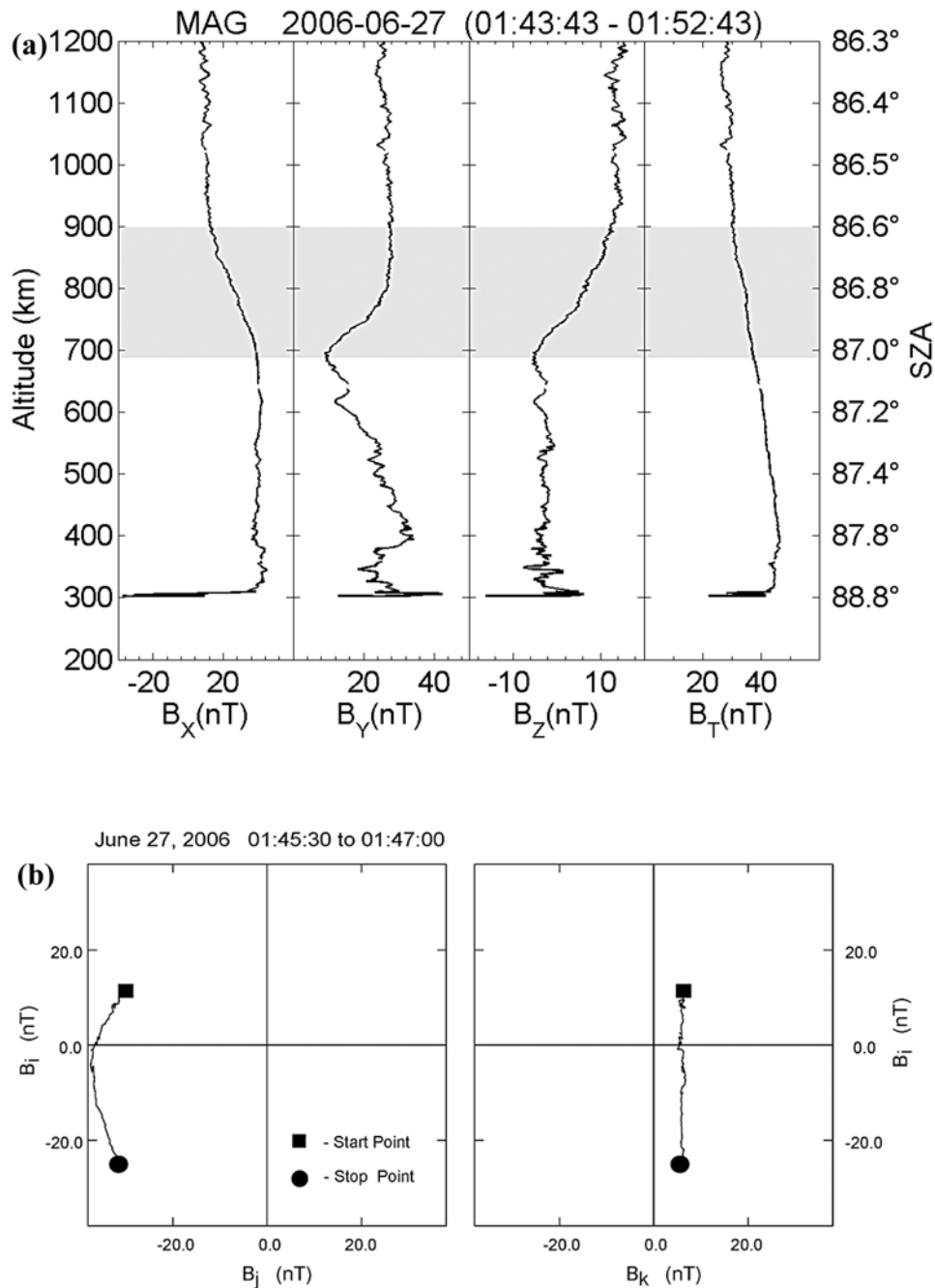


Figure 4. (a) Altitude profiles of the magnetic field components and magnitude in the inbound magnetopause crossing on 27 June 2006. MVA is applied on the shaded area. (b) Hodogram of the magnetopause crossing.

spacecraft coordinates for all three components. In the ΔB time series, all variations are caused by the spacecraft disturbances, no natural signal appears on these time series. This allows us to categorize the spacecraft disturbances using various mathematical approaches such as fuzzy logic, neural network etc. In general, there are three kinds of disturbances in the ΔB time series: jumps, regular drift variations, and irregular variations. Once all disturbances are categorized from the ΔB time series, we examine the effect of each kind of disturbance on the outboard sensor

measurements. Finally, automatic data cleaning software has been developed to remove all identified disturbances at the outboard sensor measurements and the offset determination algorithm is applied to remove the large strayfield [Leinweber *et al.*, 2008].

[9] One of the advantages of the VEX magnetometer (MAG) measurements is the higher time resolution compared with that of PVO. During a nominal 24 h VEX orbit, the MAG data are sampled at 1, 32, and 128 Hz. Initially, the sampling rate was set at 128 Hz for 2 min and 32 Hz for

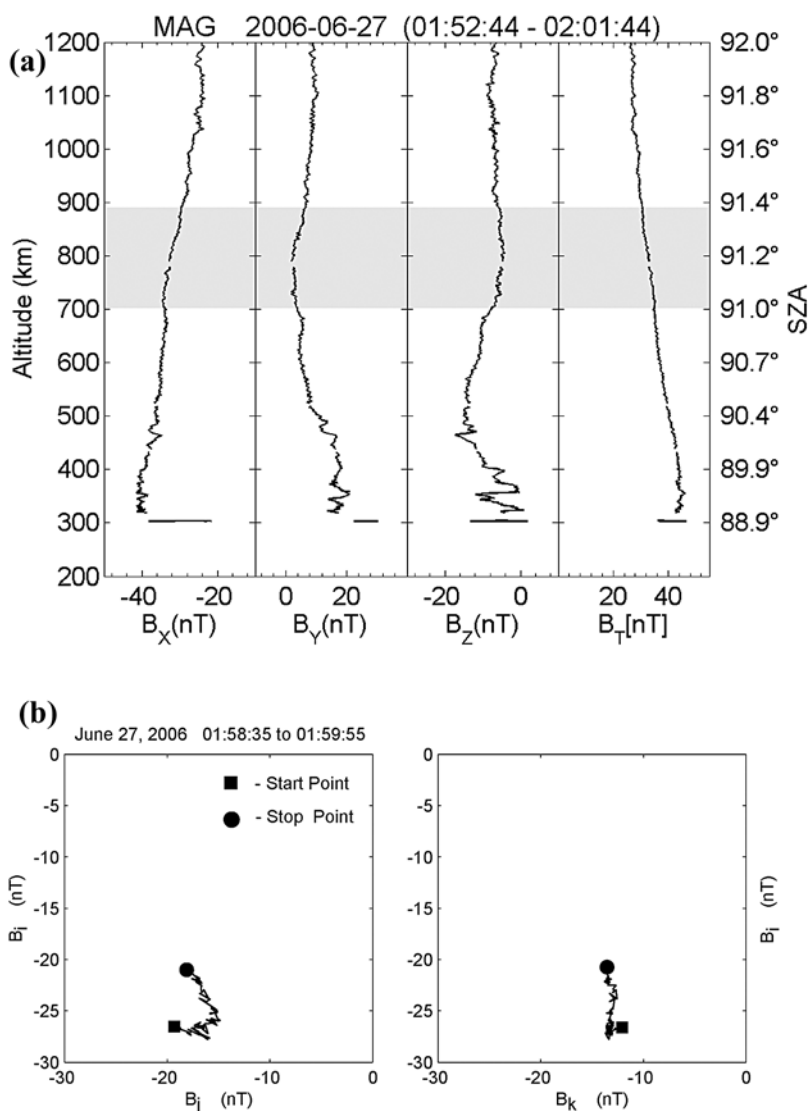


Figure 5. (a) Altitude profiles of the magnetic field components and magnitude in the outbound magnetopause crossing on 27 June 2006. MVA is applied on the shaded area. (b) Hodogram of the magnetopause crossing.

120 min around the pericenter. Later, the fast modes have been increased to 10 min for 128 Hz and 4 h for 32 Hz. Furthermore, all 128 and 32 Hz data are merged into the 1 Hz data set by applying the exact same averaging algorithm as was done onboard. So far, all 1 Hz data are cleaned with an absolute field accuracy of ~ 1 nT, and the variable field accuracy better than 0.1 nT. Thus the data are of a quality comparable to magnetic field measurements made onboard magnetically clean spacecraft.

3. Observations of Induced Magnetosphere

[10] Figure 2 displays VEX MAG measurements during a typical induced magnetosphere encounter while the interplanetary magnetic field (IMF) was very steady indicated by the little variation in both orientation and magnitude between inbound and outbound IMF. The observations are 1 Hz averages in Venus Solar Orbital (VSO) coordinates where the x axis points from Venus to the Sun, the Y axis is

opposite to the Venus orbital motion and Z axis is northward. The spacecraft moves near the terminator region, defined as where the solar zenith angle (SZA) near 90° , from dusk ($-Y$) to dawn ($+Y$), enters the magnetosheath at about 0128 UT and exits the magnetosheath at about 0232 UT. Around periaresis (0153 UT, altitude 302 km, SZA 88.8°) in the inner magnetosheath, the field is enhanced to form a magnetic barrier, the induced magnetosphere on the dayside (shaded region in the Figure 2). Apparently, the wave activity is suppressed in the magnetic barrier. Here we define the magnetopause as where the magnetosheath waves stop. Along with the cessation of wave activity at the magnetopause, the field direction exhibits an abrupt change as shown in Figure 2. Using also the dynamic power spectrum of the 32 Hz data (not shown in this paper [see Zhang *et al.*, 2007]), we identify the magnetopause crossings at 0146 UT (altitude 823 km, SZA 87°) for inbound and 0200 UT (altitude 905 km, SZA 91°) for outbound. As expected for solar minimum conditions

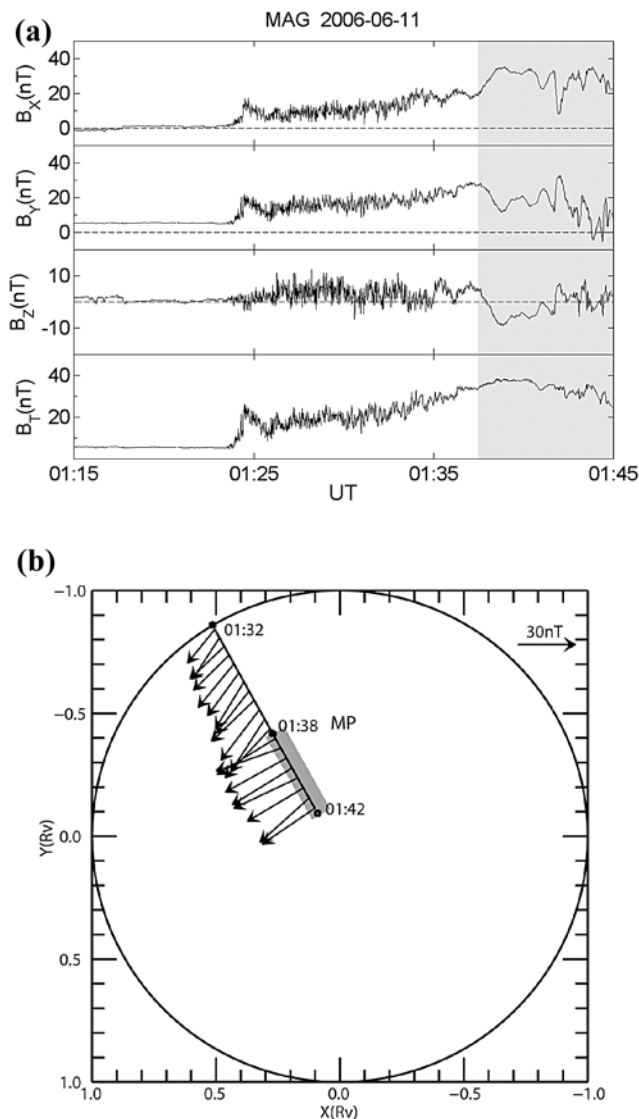


Figure 6. (a) Magnetic field observations of the induced magnetosphere and its outer boundary on 11 June 2006. (b) The magnetic field plotted along the spacecraft trajectory between 0132 and 0142 UT, 11 June 2006. The thick line marks the induced magnetosphere part of the trajectory. The magnetopause occurs at 0138 UT.

[Zhang *et al.*, 2006], no ionopause is observed for this periapsis passage since the ionopause is generally lower than the 250–350 km pericenter altitude of the spacecraft. In Figure 3 the magnetic field direction is plotted along the spacecraft trajectory. The reversal of the field in the X direction around the periapsis 0153 UT indicates the formation of the “magnetic pole” at terminator [Russell *et al.*, 1982]. In describing the geometry of an induced magnetosphere, it is common to refer the magnetic pole and “magnetic equator” with respect to the orientation of IMF. The magnetic equator lies in plane which contains the IMF. The magnetic pole is in the direction perpendicular to the magnetic equatorial plane.

[11] Clearly evident in the induced magnetosphere portion in the Figure 3 is the draping of the field lines about the

planet. We note that the inbound magnetopause crossing (0140 UT) is much better defined than the outbound magnetopause crossing (0200 UT). The reason for this difference is due to the location and nature of the magnetopause structure which we will examine in detail in the following section.

4. Magnetopause Structure

[12] The minimum variance analysis (MVA), pioneered for space magnetic field applications by *Sonnerup and Cahill* [1967], has been widely used in the determination of the normal direction of the magnetopause. Since the divergence of B is zero, the variation of B along the normal to a thin current sheet is generally small, unless there is small-scale, patchy reconnection that is easily recognized. Thus MVA allows us to estimate the normal to simple planar current sheets from magnetic field data measured with a single spacecraft. Here we also test the stability of the normal orientation determined from MVA by performing the MVA with several nested time intervals around the discontinuity and checked for a consistent result.

[13] Ideally, when the magnetic component along the current sheet normal, B_n , is zero, the current sheet can be categorized as tangential discontinuity; otherwise, it is a rotational discontinuity [Burlaga, 1969]. However, this definition is not valid when one applies MVA to determine the normal component of the current sheet using single spacecraft magnetic field measurements since the obtain B_n is never a zero number. *Lepping and Behannon* [1980] found that the ratio between B_n , obtained from MVA, and the averaged magnetic field magnitude B across the discontinuity can be used in distinguishing tangential from rotational discontinuity. They determined a threshold of $|B_n/B| = 0.3$ as the upper bound of a tangential discontinuity.

4.1. Case 1: 27 June 2006, Inbound

[14] Figure 4 shows the magnetic field altitude profile of the inbound crossing on 27 June 2006. Between ~ 700 and 900 km, the field direction changes dramatically with the tendency of B_y and B_z toward zero and increasing B_x , an indication of more draping. We apply MVA on the data between 0145:30 and 0147:00 UT, corresponding to the altitude between 898 and 685 km indicated by the shaded band in the plot. We find that the normal vector is $[0.346 \ -0.331 \ 0.878]$. The ratio of the intermediate to the minimum eigenvalues, λ_2/λ_3 , is found to be 50.1, indicating a well-defined minimum variance direction. Here we have also tested the stability of the normal orientation determined from MVA by performing the MVA with nested time intervals and the result is consistent. The magnetic field component along the minimum variance direction $B_n = 6.01$ nT and the average magnetic field magnitude across the magnetopause $B_t = 37.07$ nT. Since the ratio B_n/B_t is 0.16, which is much less the threshold of 0.3 [Lepping and Behannon, 1980], this magnetopause crossing is a tangential discontinuity.

4.2. Case 2: 27 June 2006, Outbound

[15] Figure 5 shows the magnetic field altitude profile of the outbound magnetopause crossing on 27 June 2006. The crossing is not well identified as expected for a nightside magnetopause crossing of an induced magnetosphere. We

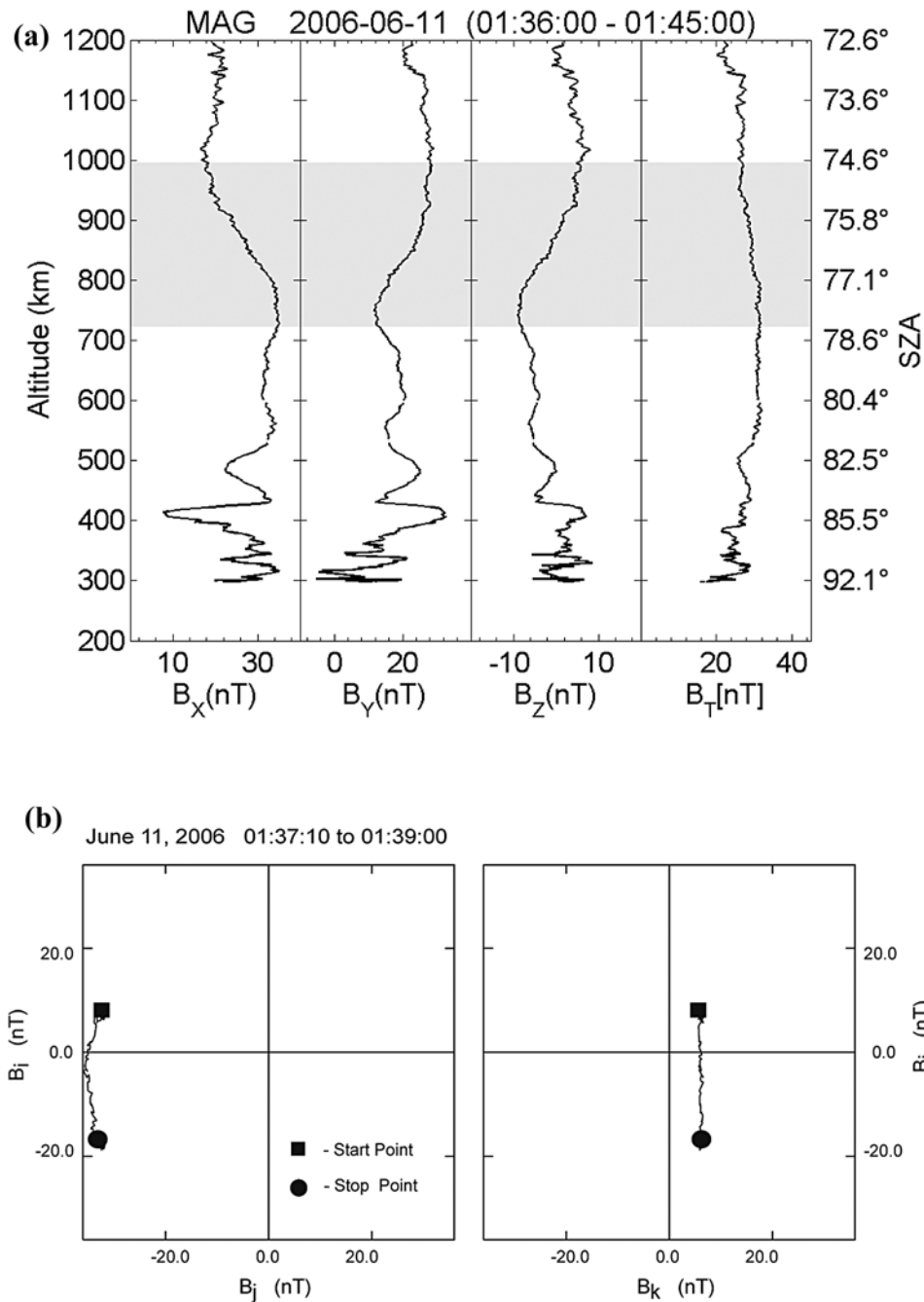


Figure 7. (a) Altitude profiles of the magnetic field measurements on 11 June 2006. MVA is applied on the shaded area. (b) Hodogram of the magnetopause crossing.

apply MVA on the data between 0158:35 and 0159:55 UT. We find that the normal vector is $[0.478 \ -0.571 \ -0.668]$, the ratio of the intermediate to the minimum eigenvalues, λ_2/λ_3 , is 11.5. Thus the minimum variance direction is well defined. Again the stability of the normal was tested with nested time interval and we found that the obtained minimum variance direction is stationary. For this magnetopause crossing, the magnetic field component along the minimum variance direction $B_n = 13.9$ nT and the average field magnitude $B_t = 32.9$ nT, the ratio is 0.42. Thus here we have a rotational discontinuity with a large field component along the normal direction.

4.3. Case 3: 11 June 2006, Inbound

[16] Figure 6a shows magnetic field time series of a well-defined magnetopause crossing at 0138 UT, 11 June 2006 (altitude 862 km, SZA 76°). Similar as in the example of 27 June 2006, the IMF is mainly in Y direction. Figure 6b shows the spacecraft trajectory and field vector along it. The magnetopause crossing is evident by the field directional change with pronounced draping. Also the wave activity clearly stops at the magnetopause. Figure 7 shows the magnetic altitude profile. We apply MVA on the data between 0137:10 and 0139:00 UT, corresponding to the altitude between 994 and 718 km indicated by the shading in the

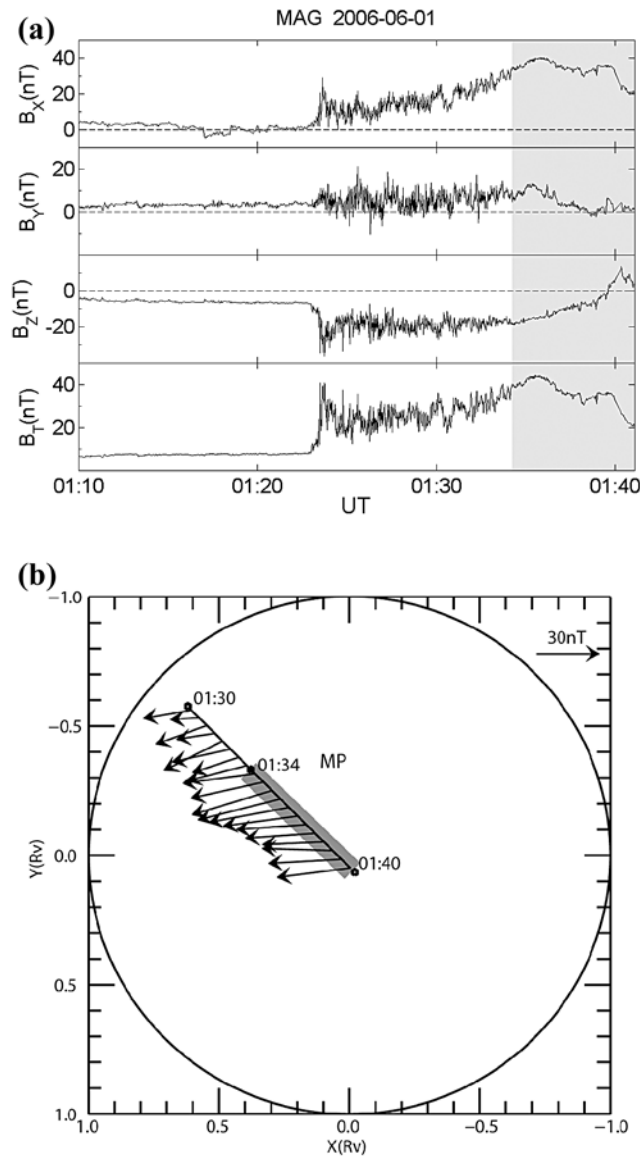


Figure 8. (a) Magnetic field observations of the induced magnetosphere and its outer boundary on 1 June 2006. (b) The magnetic field plotted along the spacecraft trajectory between 0130 and 0140 UT, 1 June 2006. The thick line marks the induced magnetosphere part of the trajectory. The magnetopause crossing occurs at 0134 UT.

plot. We find that the normal vector is $[0.046 \ -0.259 \ 0.841]$. The minimum variance direction is well defined with λ_2/λ_3 of 24.3. The magnetic field component along the minimum variance direction $B_n = 6.04$ nT and the average field magnitude $B_t = 35.93$ nT, the ratio is 0.17. Similar as case 1, this magnetopause crossing is a tangential discontinuity.

4.4. Case 4: 1 June 2006, Inbound

[17] In Figure 8a we show the inbound magnetopause crossing on 1 June 2006. One main reason to select this event is that the IMF is mainly in the Z direction. From Figures 8a and 8b, the magnetopause crossing at 0134 UT (altitude 864 km, SZA 71°) is evident by the magnetosheath wave activity abrupt ending and pronounced field draping.

We apply MVA on the data between 0134:15 and 0135:45 UT, corresponding to the altitude between 829 and 627 km indicated by the shading in Figure 9. We find that the normal vector is $[0.347 \ 0.158 \ -0.925]$ and ratio λ_2/λ_3 of 3.79. Although the minimum variance direction is not well defined from MVA in this case, the normal direction is reasonably well determined since it is normal to the expected magnetopause at solar minimum. Furthermore, we have also tested the stability of the normal orientation determined from MVA by performing the MVA with nested time intervals and the result is consistent. The magnetic field component along the minimum variance direction $B_n = 29.45$ nT and the average field magnitude $B_t = 41.5$ nT, the ratio B_n/B_t is 0.71. Thus this magnetopause crossing resemble to a rotational discontinuity.

5. Discussion and Conclusions

[18] The induced magnetosphere of Venus is a region within which the magnetic pressure dominates all other pressure contributions. It is strongest at the subsolar point and weakens with increasing solar zenith angle. Although the lower boundary of the induced magnetosphere can normally be defined by the ionopause, this is not always the case. For example, at solar minimum or at solar maximum but when the solar wind ram pressure is high, the ionosphere is fully magnetized, and the induced magnetosphere is found deeply inside the ionosphere. In such case, the lower boundary of the induced magnetosphere is below the nominal ionopause location. Furthermore, the nightside ionopause is ill-defined and so is the lower boundary of the induced magnetosphere at the nightside.

[19] In contrast to the lower boundary of the induced magnetosphere at Venus, the upper boundary, a magnetopause separating the magnetosheath solar wind plasma from the induced magnetosphere, is well defined as shown by initial Venus Express measurements [Zhang *et al.*, 2007]. While the VEX measurements characterize the magnetopause in the terminator region, previous studies show that the same magnetopause, although other names might have been given, extends both to the subsolar region and the distant magnetotail. In a study of the dimension and magnetic structure of the distant Venus magnetotail, Saunders and Russell [1986] identified the magnetopause as a directional discontinuity. By examining four unambiguous tail boundary crossings, they showed that Venus magnetopause is either a rotational or a tangential discontinuity depending on the location of the observation. They pointed out that the tangential discontinuity occurs at a plasma sheet/magnetosheath interface, whereas the rotational discontinuity occurs at a tail lobe/magnetosheath interface. Therefore, Saunders and Russell [1986] first revealed the IMF control of the magnetopause structure at the distant magnetotail.

[20] A more recent study of the structure of the magnetopause, i.e., the magnetic pileup boundary, at Mars and Venus was performed by Bertucci *et al.* [2005]. Using six magnetopause crossings both at dayside Venus and Mars, they concluded that this boundary resembles a tangential discontinuity rather than a rotational discontinuity. However, no IMF orientation control of the structure of the magnetopause was considered in their investigation.

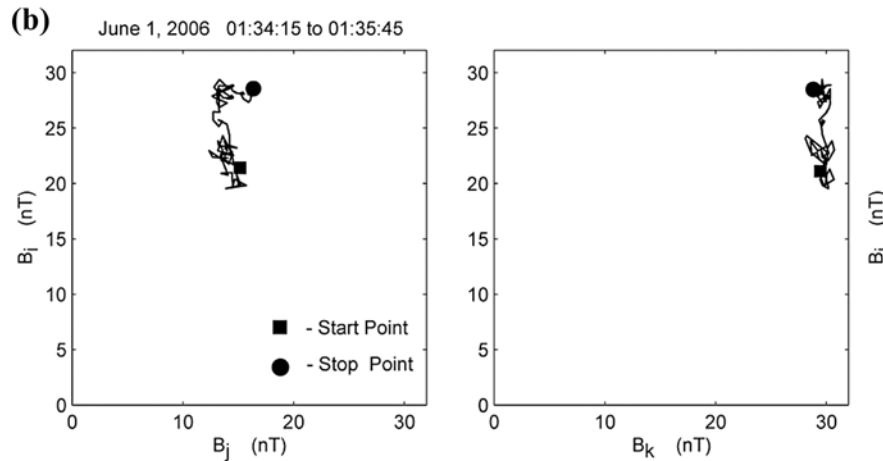
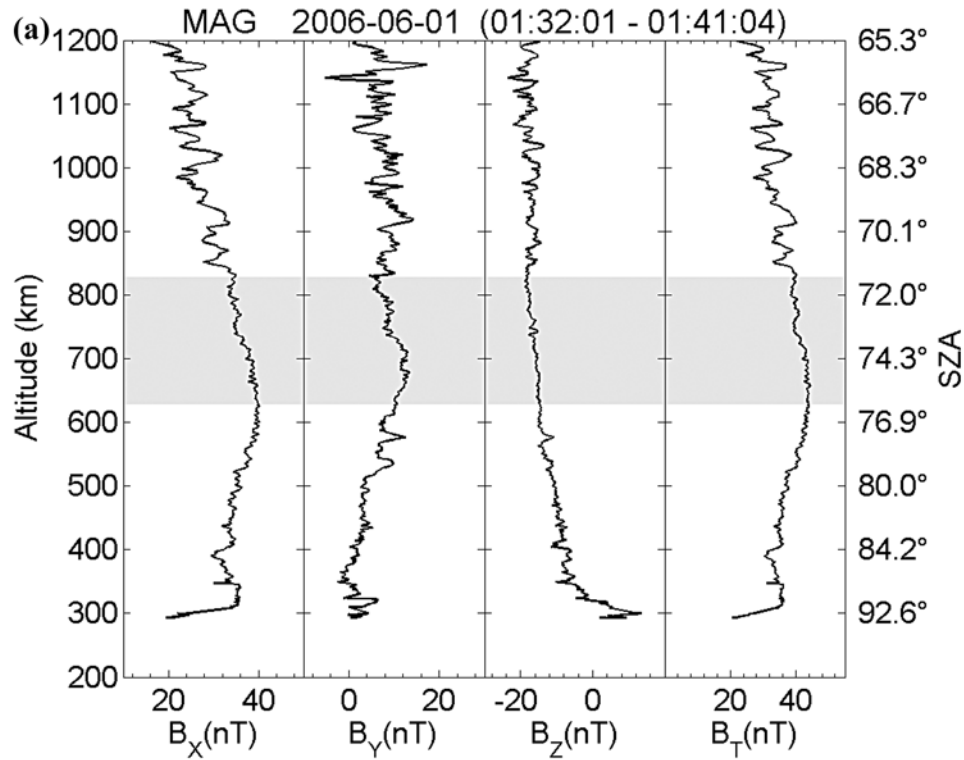


Figure 9. (a) Altitude profiles of the magnetic field measurements on 1 June 2006. MVA is applied on the shaded area. (b) Hodogram of the magnetopause crossing.

[21] In the present study, we examined four magnetopause crossings of the induced magnetosphere of Venus. We found that Venus magnetopause exhibits properties resembling both tangential and rotational discontinuity, a conclusion consistent with the results of *Saunders and Russell*

[1986], but different from the results from *Bertucci et al.* [2005]. In order to resolve this difference, we further examine the possible controlling factor of the structure of the magnetopause. In Table 1, we list the magnetopause crossing location and the IMF conditions. Further we list the

Table 1. Magnetopause Crossing Locations and IMF Conditions

Case	Magnetopause Crossing in VSO (km)	IMF (nT)	Altitude (km)	SZA	Clock Angle	Magnetopause Structure
1	390 -2853 6245	-0.18 7.94 0.97	823	87°	108°	tangential
2	-177 4895 4940	0.11 8.69 2.05	905	91°	32°	rotational
3	1645 -2535 6219	0.73 5.20 -0.18	862	76°	114°	tangential
4	2284 -2007 6213	0.48 3.84 -6.62	864	71°	168°	rotational

altitude, the SZA and the clock angle of the magnetopause crossing. The clock angle is defined as the angle between the radius vector to the spacecraft at the magnetopause and the IMF both projected in the YZ plane. At terminator region, it is usual to call a clock angle of 90° or -90° as the magnetic pole and a clock angle of 0° or 180° as the magnetic equator. Because of the VEX orbital geometry, our magnetopause examples are limited to the terminator region covering a SZA between 71° to 91° . From Table 1, we can see that the magnetopause in a magnetic pole region exhibits properties of a tangential discontinuity, whereas a rotational discontinuity is found for a magnetopause at the magnetic equator. Therefore, it is evident that the IMF orientation exerts strong control on the structure of the magnetopause of the induced magnetosphere at Venus.

[22] Ideally, the magnetopause is defined as pressure-balanced boundary where the magnetic pressure in the induced magnetosphere equals the ram pressure of the magnetosheath solar wind. However, due the insufficient temporal resolution of the PVO plasma instrument, such a definition could not be applied to data analysis in practice. A modified pressure balance boundary definition was proposed by Zhang *et al.* [1991] to determine the outer boundary of the magnetic barrier as the altitude where the magnetosheath magnetic pressure is equal half of the upstream solar wind dynamic pressure. Indeed, initial analysis of the ASPERA data shows that the so-called ion composition boundary [Martinecz *et al.*, 2008] is collocated with the magnetopause. When the combined plasma and magnetic field data set is available, we plan to investigate the pressure balance nature of the magnetopause.

[23] **Acknowledgments.** The work at China was supported by CAS grant KJCX2-YW-T13 and NNSFC grants 40621003 and 40628003. The work at UCLA was supported by the National Aeronautics and Space Administration under research grant NNG06GC62G. The work in Slovakia was supported by Slovak Research and Development Agency under the contract APVV-51-053805.

References

- Barabash, S., *et al.* (2007), The loss of ions from Venus through the plasma wake, *Nature*, *450*, 650–653, doi:10.1038/nature06434.
- Bertucci, C., C. Mazelle, M. H. Acuna, C. T. Russell, and J. A. Slavin (2005), Structure of the magnetic pileup boundary at Mars and Venus, *J. Geophys. Res.*, *110*, A01209, doi:10.1029/2004JA010592.
- Burlaga, L. F. (1969), Directional discontinuities in the interplanetary magnetic field, *Sol. Phys.*, *7*, 54–71, doi:10.1007/BF00148406.
- Fedorov, A., *et al.* (2008), Comparative analysis of Venus and Mars magnetotails, *Planet. Space Sci.*, *56*, 812–817, doi:10.1016/j.pss.2007.12.012.
- Kallio, E., *et al.* (2008), The Venusian induced magnetosphere: A case study of plasma and magnetic field measurements on the Venus Express mission, *Planet. Space Sci.*, *56*, 796–801, doi:10.1016/j.pss.2007.09.011.
- Leinweber, H. K., C. T. Russell, K. Torkar, T. L. Zhang, and V. Angelopoulos (2008), An advanced approach to finding magnetometer zero levels in the interplanetary magnetic field, *Meas. Sci. Technol.*, *19*(5), 055104, doi:10.1088/0957-0233/19/5/055104.
- Lepping, R. P., and K. W. Behannon (1980), Magnetic field directional discontinuities: 1. Minimum variance errors, *J. Geophys. Res.*, *85*, 4695–4703, doi:10.1029/JA085iA09p04695.
- Luhmann, J. G., S. A. Ledvina, and C. T. Russell (2004), Induced magnetospheres, *Adv. Space Res.*, *33*, 1905–1912, doi:10.1016/j.asr.2003.03.031.
- Martinecz, C., *et al.* (2008), Location of the bow shock and ion composition boundaries at Venus: Initial determinations from Venus Express ASPERA-4, *Planet. Space Sci.*, *56*, 780–784, doi:10.1016/j.pss.2007.07.007.
- Ness, N. F., K. W. Behannon, R. P. Lepping, and K. H. Schatten (1971), Use of two magnetometers for magnetic field measurements on a spacecraft, *J. Geophys. Res.*, *76*, 3565–3573.
- Ness, N. F., M. H. Acuna, K. W. Bahannon, and F. M. Neubauer (1982), The induced magnetosphere of Titan, *J. Geophys. Res.*, *87*, 1369–1381, doi:10.1029/JA087iA03p01369.
- Podgorny, I. M., E. M. Dubinin, and P. L. Israelevich (1980), Laboratory simulation of the induced magnetospheres of Comets and Venus, *Earth Moon Planets*, *23*, 323–338, doi:10.1007/BF00902047.
- Russell, C. T., R. C. Elphic, and J. A. Slavin (1979), Initial Pioneer Venus magnetic field results: Dayside observations, *Science*, *203*, 745–748, doi:10.1126/science.203.4382.745.
- Russell, C. T., J. G. Luhmann, R. C. Elphic, F. L. Scarf, and L. H. Brace (1982), Magnetic field and plasma wave observations in a plasma cloud at Venus, *Geophys. Res. Lett.*, *9*, 45–48, doi:10.1029/GL009i001p00045.
- Saunders, M. A., and C. T. Russell (1986), Average dimension and magnetic structure of the distant Venus magnetotail, *J. Geophys. Res.*, *91*, 5589–5604, doi:10.1029/JA091iA05p05589.
- Sonnerup, B. U. Ö., and L. J. Cahill (1967), Magnetopause structure and attitude from Explorer 12 observations, *J. Geophys. Res.*, *72*, 171–183, doi:10.1029/JZ072i001p00171.
- Titov, D. V., *et al.* (2006), Venus Express science planning, *Planet. Space Sci.*, *54*, 1279–1297, doi:10.1016/j.pss.2006.04.017.
- Zhang, T. L., J. G. Luhmann, and C. T. Russell (1991), The magnetic barrier at Venus, *J. Geophys. Res.*, *96*, 11,145–11,153, doi:10.1029/91JA00088.
- Zhang, T. L., *et al.* (2006), Magnetic field investigation of the Venus plasma environment: Expected new results, *Planet. Space Sci.*, *54*, 1336–1343, doi:10.1016/j.pss.2006.04.018.
- Zhang, T. L., *et al.* (2007), Little or no solar wind enters Venus' atmosphere at solar minimum, *Nature*, *450*, 654–656, doi:10.1038/nature06026.
- Zhang, T. L., *et al.* (2008a), Initial Venus Express magnetic field observations of the magnetic barrier at solar minimum, *Planet. Space Sci.*, *56*, 790–795, doi:10.1016/j.pss.2007.10.013.
- Zhang, T. L., *et al.* (2008b), Initial Venus Express magnetic field observations of the Venus bow shock location at solar minimum, *Planet. Space Sci.*, *56*, 785–789, doi:10.1016/j.pss.2007.09.012.
- H.-U. Auster, Institut für Geophysik und Extraterrestrische Physik, Technische Universität, Mendelssohnstrasse 3, D-38106 Braunschweig, Germany.
- M. Balikhin, Department of Automatic Control and Systems Engineering, University of Sheffield, Mappin Street, Sheffield S1 3JD, UK.
- S. Barabash, Swedish Institute of Space Physics, Box 812, SE-98128 Kiruna, Sweden.
- W. Baumjohann, M. Delva, M. Volwerk, and T. L. Zhang, Space Research Institute, Austrian Academy of Sciences, A-8042 Graz, Austria. (tielong.zhang@oeaw.ac.at)
- K. Kudela, Institute of Experimental Physics, Slovak Academy of Sciences, Watsonova 47, 040 01 Košice, Slovakia.
- C. T. Russell and H. Y. Wei, Institute of Geophysics and Planetary Physics, University of California, Los Angeles, CA 90095, USA.
- C. Wang, State Key Laboratory of Space Weather, Center for Space Science and Applied Research, Chinese Academy of Sciences, Beijing 100080, China.